Accurate circuit analysis of resonant-type left handed transmission lines with inter-resonator coupling

Cite as: J. Appl. Phys. **100**, 074908 (2006); https://doi.org/10.1063/1.2353174
Submitted: 10 February 2006 . Accepted: 26 June 2006 . Published Online: 10 October 2006

I. Gil, J. Bonache, M. Gil, J. García-García, F. Martín, and R. Marqués

Accurate circuit analysis of resonant-type left handed transmission lines with inter-resonator coupling

I. Gil,[a),b)] J. Bonache, M. Gil, J. García-García, and F. Martín[a),c)]
Departament d'Enginyeria Electrònica, Universitat Autònoma de Barcelona, 08193 Bellaterra (Barcelona), Spain

R. Marqués[d)]
Departamento de Electrónica y Eletromagnetismo, Facultad de Física, Universidad de Sevilla, Avendia Reina Mercedes s/n, 41012 Sevilla, Spain

(Received 10 February 2006; accepted 26 June 2006; published online 10 October 2006)

In this paper, a circuit model for the description of left handed transmission lines based on complementary split rings resonators (CSRRs) is proposed. As compared to previous models, coupling between adjacent resonators is included in the present work. The conditions that make this coupling significant are discussed. Specifically, it will be shown that it is barely present when circular CSRRs are used to implement the left handed transmission line. However, if the line is loaded with rectangular CSRRs separated by a small distance, inter-resonator coupling is important and it significantly influences the electromagnetic behavior of the structures. It will be also shown that under low or moderate coupling, it is possible to describe the structures by means of a simplified model with modified parameters. Several prototype devices with different CSRR topologies and coupling levels have been fabricated to illustrate the phenomenology associated with these structures and the accuracy of their model descriptions. The results of this work can be of interest for the design of planar microwave circuits based on CSRR left handed lines. © *2006 American Institute of Physics*. [DOI: 10.1063/1.2353174]

I. INTRODUCTION

From the experimental demonstration of left handedness by Smith *et al.* in 2000,[1] the number of works devoted to the synthesis of left handed media (LHM) in one,[2–5] two,[6,7] and three dimensions,[8] to the demonstration of their exotic electromagnetic properties (including negative refraction[9–11] and subwavelength focusing,[12–16] among others), and to point out their potential engineering applications[17] (mainly in the microwave range of the electromagnetic spectrum) has dramatically increased. LHM do not exist in nature, but they can be artificially synthesized and belong to the category of the so-called metamaterials, which are considered to be a *hot research topic* at present days. Metamaterials are artificially fabricated composites of small constitutive elements (*atoms*) or inclusions that make the structure to behave as an effective (continuous) medium with electromagnetic properties different than those of their constitutive atoms (and usually not found in natural media). In particular, LHM exhibit negative values of the effective permittivity ε and permeability μ. The properties of these substances were already pointed out by Veselago in 1968.[18] These properties (including negative refraction, inversion of the Doppler effect, Cerenkov radiation, and Goos-Hänchen effect) are indeed consequence of the antiparallelism between the phase and group velocities for propagating waves in such media. Namely, due to the negative values of ε and μ, the electric field intensity vector $\boldsymbol{E}$, the magnetic field intensity vector $\boldsymbol{H}$, and the propagating vector $\boldsymbol{k}$ form a left handed triplet, and energy flow (given by the Poynting vector) and group velocity are contradirectional to wave propagation. Although the work by Veselago was considered as theoretical speculation during years, it is nowadays quoted in most metamaterial journal papers and conference proceedings, and it is believed that metamaterials can have a significant impact in several fields of science and engineering. Several patents in the area of communications technology have been recently proposed or are under exploitation, this being indicative of the potentiality of metamaterials in future.

For the fabrication of the former LHM,[1] Smith *et al.* made use of metallic posts and nonmagnetic resonant particles, namely, split rings resonators (SRRs) (see Fig. 1).[19] They combined both elements to generate a periodic structure with the characteristics of a continuous medium. The metallic posts made the structure to behave as an electric plasma scaled down to microwave frequencies. Thus, a negative effective permittivity was artificially generated up to a

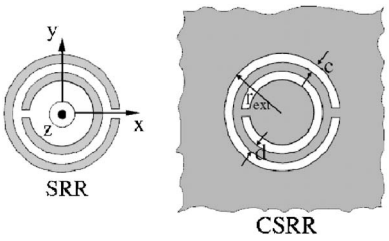

FIG. 1. Geometries of the SRR and the CSRR. Gray zones represent the metallization.

[a)]FAX: 34 93 581 26 00.
[b)]Electronic mail: nacho.gil@uab.es
[c)]Electronic mail: ferran.martin@uab.es
[d)]Electronic mail: marques@us.es

cutoff (or plasma) frequency, dependent on the distance between posts and their radius. The required negative permeability to form a LHM came from the presence of the SRRs. For incident radiation polarized with the magnetic field parallel to the rings' axis (z axis), SRRs provide a negative value of the magnetic permeability in a narrow band above resonance. Thus, as long as the post-related plasma frequency is set beyond the resonance frequency of the SRRs, there is a region where negative ε and μ simultaneously coexist.[1] A key aspect to achieve a continuous medium is the small electrical size of SRRs. Thanks to the high electric coupling between the concentric rings forming the SRR (which can be enhanced by merely reducing the inter-rings space or by using alternative topologies[20–22]), it is possible to drive the first resonance of the *particle* to small values (as compared to the resonant frequency of the individual open rings).[23] In other words, SRRs can be made physically small at the desired frequency (resonance frequency), this being a necessary condition for the synthesis of an effective (or continuous) medium.

Due to the small electrical size of their constitutive elements, metamaterials and other structures based on them can be of interest for the design of functional devices with small dimensions. Specifically, in microwave engineering, most planar circuits and devices are based on transmission lines and stubs, their dimensions scale with the operating frequency, and they are sometimes too huge for practical applications.[24] Therefore, metamaterials are of interest in this area in order to achieve high levels of miniaturization for devices and circuits. Since many microwave and telecommunication applications should be compatible with planar technology, the synthesis of one-dimensional planar metamaterials (and left handed structures, in particular) has been a natural demand. In this regard, two main approaches have been followed: (i) those based on resonant-type constitutive elements, such as SRRs, and (ii) those based on the dual transmission line concept. Chronologically, the latter approach was formerly proposed, and it was done almost simultaneously by Oliner,[2] Caloz and Itoh,[3] and Grbic and Eleftheriades.[4] A dual transmission line is simply a one-dimensional propagating medium that can be described by an equivalent circuit model that is the dual of that circuit modeling a conventional transmission line. Namely, capacitors are series connected, whereas inductors are placed in shunt configuration. By taking into account that plane wave propagation in homogeneous isotropic media and transverse electromagnetic (TEM) propagation in transmission lines are described by equivalent equations, we can identify a negative effective permittivity and permeability for the dual transmission line given by $\varepsilon=-(\omega^2 L)^{-1}$ and $\mu=-(\omega^2 C)^{-1}$.[4] Therefore, the series capacitors are responsible for the negative effective permeability, whereas the shunt connected inductors provide the negative valued permittivity to the dual transmission line. However, in practice, a host transmission line is required to physically implement a dual transmission line. The parasitic elements of this line must be taken into account for an accurate description of the structure, which has been termed as composite right/left handed (CRLH) transmission line, since it exhibits typically two frequency regions (or allowed bands): one with left handed wave propagation and the other being dominated by the elements of the host line and thus exhibiting forward wave propagation.[25,26] The CRLH concept has been applied by Caloz and Itoh to the design of many functional devices and circuits at microwave frequencies (see their recently published monographic book on metamaterials[17]). The resonant-type approach was initially proposed by Martín *et al.*,[27] and it was inspired by the left handed structure proposed by Smith *et al.*.[1] SRRs were etched in the back substrate side of a coplanar waveguide structure, while the metallic posts of the Smith medium were substituted by shunt connecting metallic wires between the central strip and the ground plane. The latter can be modeled as shunt inductors, thus providing the negative effective permittivity to the structure (as for the dual transmission lines). Alternatively to these SRR based left handed transmission lines, a technique for the synthesis of left handed lines was proposed by Falcone *et al.*,[28] where the negative permittivity (rather than permeability) was achieved by means of a type of resonant elements: the complementary split rings resonators (CSRRs).[29] These resonators (see Fig. 1) are the negative image of SRRs and hence are their dual counterparts. As discussed in Ref. 29, by etching CSRRs in the ground plane of a microstrip line, underneath the conductor strip, a negative effective permittivity was achieved in a narrow band in the vicinity of the resonant frequency (as revealed by the presence of a stop band in the measured frequency response). The reason for etching CSRRs under the strip is just to enhance electric coupling between the line and the CSRRs. Namely, since these elements are the dual of SRRs, they are mainly (although not exclusively) excited by an axial time varying electric field (rather than magnetic field).[30] Regarding the negative effective permeability, required to implement a left handed medium, it was achieved by etching capacitive gaps in the conductor strip, above the position of the CSRRs. These gaps make the structure to behave as a magnetic plasma, with negative permeability up to a frequency that depends on gap dimensions and distance. Hence the CSRR/gap combination is indeed the dual of the SRR/wire combination, and it is possible to fabricate resonant-type left handed transmission lines by using both resonant elements.

We would like to mention that the former planar left handed structures based on SRRs and CSRRs were implemented in coplanar waveguide (CPW) and microstrip technology, respectively. However, it has been demonstrated that left handedness can be achieved by using both resonators, regardless of the host transmission medium considered (microstrip, CPW, etc.).[31] This allows for certain flexibility in the design of microwave devices based on these structures. In this regard, it is very important to have accurate circuit models of the structures, able to describe the main physical phenomena involved. In this paper, a detailed circuit analysis of CSRR-based left handed transmission lines is carried out. As compared to previous models,[30] coupling between adjacent resonators is included in the present work, and the conditions that make this coupling significant are discussed. In Sec. II, the complete equivalent circuit model of the structures is proposed and justified. By means of several circuit equivalences it will be shown that this model can be trans-

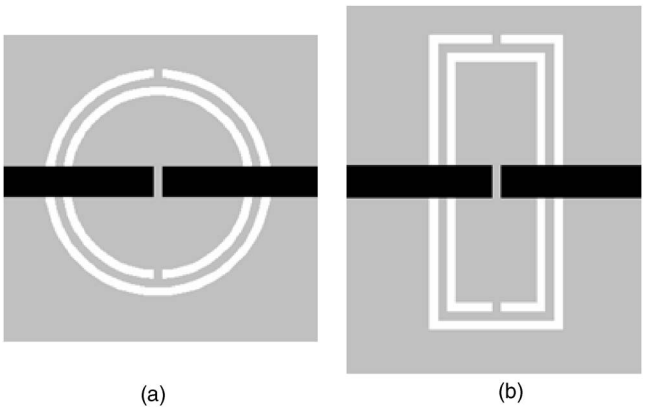

FIG. 2. Layout of the basic unit cell of the CSRR-based left handed transmission lines for circular- (a) and rectangular-shape (b) geometries. Black zones correspond to the upper metal level (conductor strip). The ground plane, where CSRRs are printed, is depicted in gray.

formed, and under certain conditions (moderate or low coupling) it can be expressed as a simplified model with modified element values. Section III is aimed at demonstrating the accuracy of the model. Comparison between results inferred from the circuit model and measurements carried out on fabricated prototypes will be given, including the analysis of the influence of inter-resonator distance when coupling must be considered. The situation corresponding to very weak coupling (large distance between resonators), as well as the influence of CSRR shape (circular or rectangular) on the frequency response, will be analyzed in Sec. IV. In Sec. V, the validity of the simplified model to describe structures with arbitrary number of cells is discussed, and the dispersion relation is obtained analytically. Finally the main conclusions of the work will be highlighted in Sec. VI.

II. ELECTRICAL MODEL OF CSRR-BASED LEFT HANDED TRANSMISSION LINES

The structure under study is a left handed transmission line implemented by means of a periodic array of CSRRs and capacitive gaps. As a host medium, a microstrip transmission line is considered in this work, as was recently done by some of the authors to study the resonances and polarizabilities of SRRs.[23] It is consists of a dielectric slab (substrate) with a metallic film on one side (ground plane) and a metallic (conductor) strip on the opposite side. By feeding one of the ports, a quasi-TEM signal propagates through the line to the output port. The basic cell of the CSRR-based LH microstrip line is depicted in Fig. 2. The series gaps are etched in the conductor strip, above the position of the CSRRs, which are etched in the ground plane. If the capacitive gaps were present alone, signal propagation would be inhibited up to a cutoff frequency f_c due to the negative effective permeability of the structure (as indicated before). However, due to the presence of the CSRRs, a frequency band that supports backward waves arises below f_c, since μ and ε are simultaneously negative in the vicinity of CSRR resonance.

The lumped element equivalent circuit model of the structure is depicted in Fig. 3. It is an improved version of a previous model reported by some of the authors,[30] where not

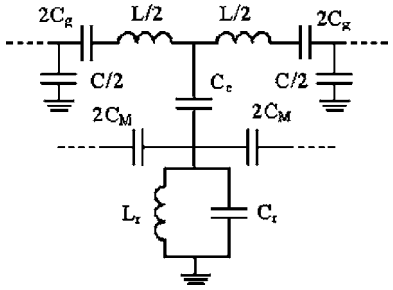

FIG. 3. Lumped element equivalent circuit model for the structures depicted in Fig. 2.

only the presence of the CSRRs and gaps, as well as CSRR-to-line coupling, is accounted for but also inter-resonator coupling and the parameters of the host line are taken into account. By these means, an accurate description of the physical behavior of the artificial line is obtained, as will be shown later. The reason to neglect coupling between adjacent resonators in previous works by the authors is simple: it was not significant because circular CSRRs were considered. However, coupling can be enhanced by using rectangular-shape CSRRs (as will be demonstrated), and for certain applications such coupling can be of interest. On the other hand, line parameters are considered in this work in order to obtain a good description of the structure beyond the left handed band and to properly describe those situations were inter-resonator coupling is very weak and the distance between CSRRs is considerable (so that transmission line effects are important). The physical meaning of the electrical parameters of Fig. 3 is as follows: L_r and C_r model the CSRRs, which are electrically coupled to the line through the capacitance C_c. The series gaps are described by the capacitance C_g, whereas L and C are the line inductance and capacitance, respectively, of the elemental cell. Finally, inter-resonator coupling is modeled by means of the mutual capacitance C_M.

Inter-resonator coupling was previously studied by some of the authors to describe the propagation of electroinductive waves (EIWs) in chains of CSRRs.[32] Actually EIW are guided waves that can be considered dual to the so-called magnetoinductive waves (MIWs), which can be generated in a periodic array of magnetically coupled resonators.[33–35] In Ref. 36, the copropagation of MIW and electromagnetic waves in the same one-dimensional system under different conditions was considered. In the present work, rather than considering the propagation of EIW (or MIW), we study signal propagation in a left handed medium composed of coupled CSRRs (rather than SRRs). It will be shown that the structure can be viewed as if no inter-resonator coupling was present, and under certain conditions (moderate or low coupling), the equivalent circuit shown in Fig. 3 can be simplified to that model reported in Ref. 30, with modified parameters.

Let us now consider a two-stage structure described by the model of Fig. 3 and two different situations corresponding to (i) small inter-resonator distance and (ii) significant separation between adjacent CSRRs. In the former case, the

line capacitance C can be neglected. From the Δ-Y equivalence and after some intermediate (and tedious) transformations, the circuit can be finally expressed as shown in Fig. 4 (see Appendix). According to this circuit, the structure can be described by a model similar to that reported in Ref. 30, namely, by excluding coupling between adjacent CSRRs, but with the series impedance modified. Specifically, this impedance is given by

$$Z_{\mathrm{eq}} = \frac{1}{j\omega C_g} \frac{[1 - L_r(C_C + 2C_M + C_r)\omega^2][L_r(C_C + C_r)\omega^2 - 1]}{LL_r^2 C_C^2 C_M \omega^6 + [1 - L_r(C_C + 2C_M + C_r)\omega^2][L_r(C_C + C_r)\omega^2 - 1] - L_r^2 C_C^2 C_M \omega^4 / C_g} + j\omega L \frac{\omega C_g [1 - L_r(C_C + 2C_M + C_r)\omega^2][L_r(C_C + C_r)\omega^2 - 1]}{LL_r^2 C_C^2 C_M C_g \omega^7 + \omega C_g [1 - L_r(C_C + 2C_M + C_r)\omega^2][L_r(C_C + C_r)\omega^2 - 1] - L_r^2 C_C^2 C_M \omega^5}, \quad (1)$$

where the first term of the right hand side of (1) corresponds to a frequency dependent capacitance $C'(\omega)$ and the second term to a frequency dependent inductance $L'(\omega)$ [see Fig. 4(g)]. The other electrical parameters of the structure are not altered by this transformation. Under moderate or low coupling, we can evaluate the impedance given by (1) at the center of the interval where propagation is allowed, and from it we can obtain effective element values, L_{eff} and C_{eff} (Fig. 5). By doing this, we do not expect a significant modification of the electrical response of this equivalent circuit model, unless the mutual capacitance is considerable. This is corroborated in Fig. 6, where we compare the electrical response of the circuit of Fig. 4(a) and the circuit of Fig. 5 for different values of C_M (parameter values are indicated in the caption). The agreement is good up to a coupling level characterized by C_M=0.2 pF, which is even higher than the maximum achievable values of mutual capacitances in actual left handed lines based on rectangular CSRRs. The parameter values indicated in Fig. 6 are arbitrary, since they do not correspond to any specific topology. However, in the next section, a method to infer these parameters from measurement or full wave simulation of CSRR-based devices will be pointed out.

For structures with CSRRs separated enough, C_M is negligible, but C increases and must be taken into account for accurate description of the left handed medium, as will be shown in Sec. IV.

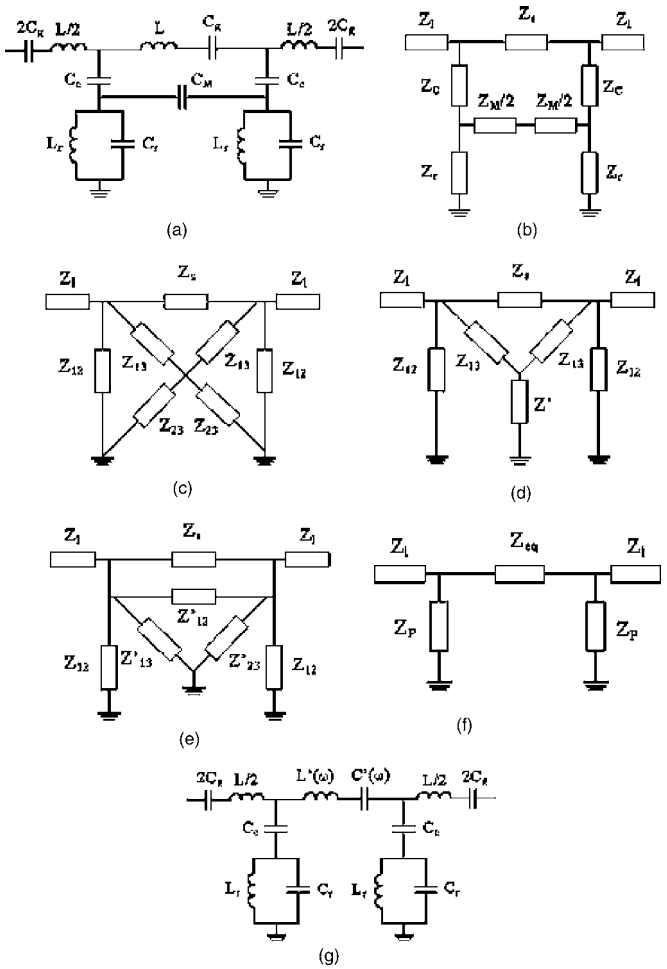

FIG. 4. Lumped element equivalent circuit for a two-stage CSRR-based left handed structure with small inter-resonator distance (g). The different steps [(a)–(f)] in the sequence illustrated are referred to in the Appendix.

III. COMPARISON TO EXPERIMENTAL DATA: MODERATE COUPLING

We have fabricated a single cell CSRR/gap prototype that has been used to determine the electrical parameters (with the exception of the mutual capacitance C_M). The layout is shown in Fig. 7, and the measured transmission coefficient from port 1 to port 2 (S_{21}) is depicted in Fig. 8 (the vector network analyzer Agilent 8720ET has been employed). The device has been fabricated on a Rogers RO3010 substrate (dielectric constant ε_r=10.2, thickness h =1.27 mm) by using a LPKF HF100 drilling machine. The

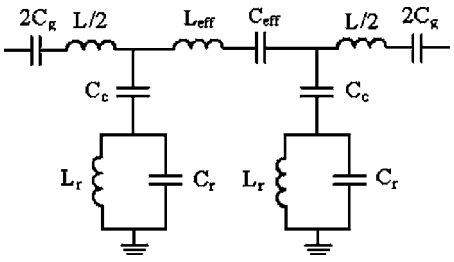

FIG. 5. Simplified model for the structures based on the cells depicted in Fig. 2.

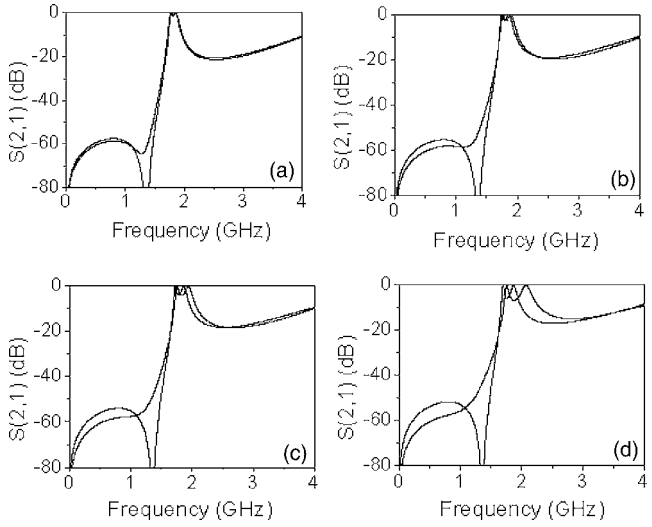

FIG. 6. Comparison of the transmission coefficient obtained from electrical simulation of the circuits shown in Fig. 4(a) (bold line) and Fig. 5 (thin line). Electrical values are L_r=1.6 nH, C_r=4.1 pF, C_c=4.6 pF, C_g=0.29 pF, L=4.9 nH, and (a) C_M=0.05 pF, L_{eff}=4.21 nH, and C_{eff}=0.34 pF; (b) C_M=0.15 pF, L_{eff}=3.26 nH, and C_{eff}=0.45 pF; (c) C_M=0.25 pF, L_{eff}=2.7 nH, and C_{eff}=0.54 pF; (d) C_M=0.5 pF, L_{eff}=1.97 nH, and C_{eff}=0.73 pF.

transmission coefficient that has been obtained by full wave electromagnetic simulation by using the commercial tool Agilent MOMENTUM is also depicted in Fig. 8. Good agreement between the experimental data and simulated results has been obtained. The parameters of the electrical circuit model have been determined by following the procedure described in Ref. 37. Namely, L and C_g have been obtained from the impedance seen from the input port at the intrinsic resonant frequency of the CSRR (which can be determined from the intersection of the reflection coefficient expressed in a Smith Chart to the normalized unity resistance circle). At this frequency, the shunt admittance is roughly zero, and hence the input impedance is the series connection of L and C_g plus the termination impedance of the output port (50 Ω). Since the line inductance L can be easily obtained from a transmission line calculator (Agilent Line Calc), the gap capacitance can be thus inferred. To extract L_r, C_r, and C_c, we have used the intrinsic resonance frequency of the CSRRs f_o given by

$$f_o = \frac{1}{2\pi\sqrt{L_r C_r}} \tag{2}$$

and the transmission zero frequency that nulls the shunt impedance and is given by

$$f_z = \frac{1}{2\pi\sqrt{L_r(C_c + C_r)}}. \tag{3}$$

These frequencies can be easily identified from the simulated or measured frequency response. A third condition is necessary to univocally determine these parameters. This comes from the phase shift of the structure (single cell), which is given by[38]

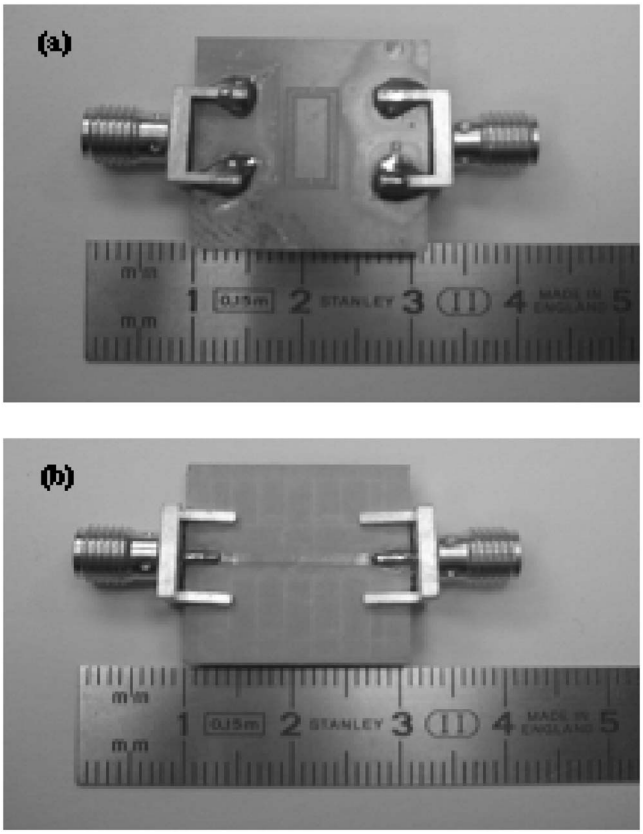

FIG. 7. Fabricated single cell CSRR microstrip line: (a) ground plane side of the substrate and (b) upper substrate side. Dimensions of rectangular CSRR are $c=d$=0.3 mm, width=10 mm, height=4.6 mm; the gap distance is 0.3 mm.

$$\cos\phi = 1 + \frac{Z_s(j\omega)}{Z_p(j\omega)}. \tag{4}$$

At the frequency where the phase shift is $\phi=\pi/2$, the series and shunt impedances must satisfy $Z_s=-Z_p$. Hence we have the third necessary condition to determine the electrical parameters of the shunt impedance, since this frequency can be easily identified from simulation or measurement. By using this method we have inferred the electrical parameters of the model (L_r=1.6 nH, C_r=4 pF, C_c=4.6 pF, C_g=0.26 pF, and L=4.4 nH), and they have been used to obtain the electrical frequency response by means of the Agilent ADS simulator

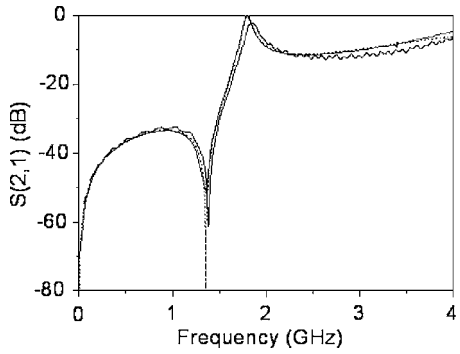

FIG. 8. Transmission coefficient for the circuit of Fig. 7. Experimental response (bold line), full wave electromagnetic simulation (thin line), and electrical simulation by using the model shown in Fig. 5 (dotted line) are depicted. L_r=1.6 nH, C_r=4 pF, C_c=4.6 pF, C_g=0.26 pF, and L=4.4 nH.

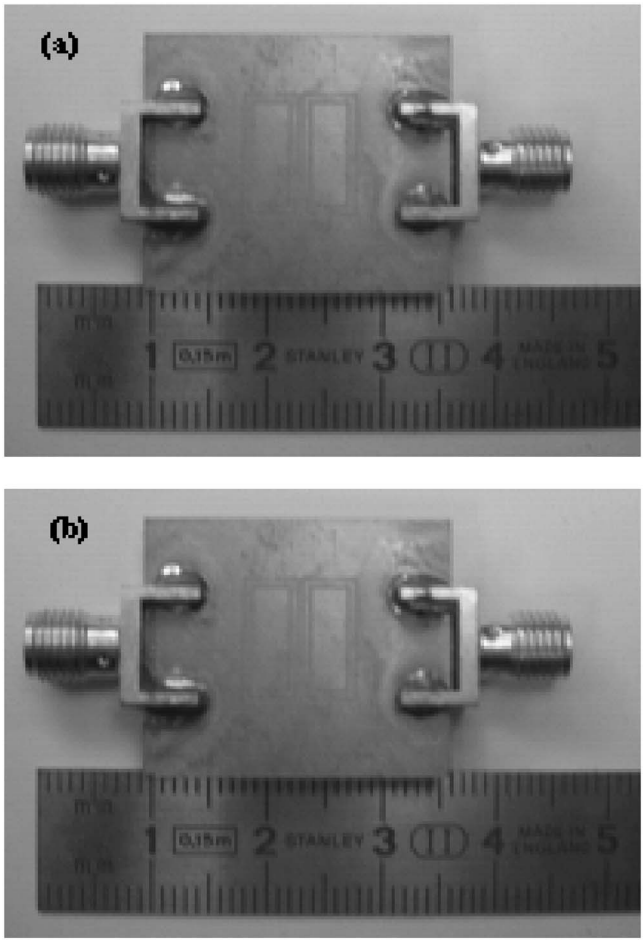

FIG. 9. Fabricated two-stage CSRR-based structures with rectangular CSRRs separated by 0.1 mm (a) and 0.2 mm (b).

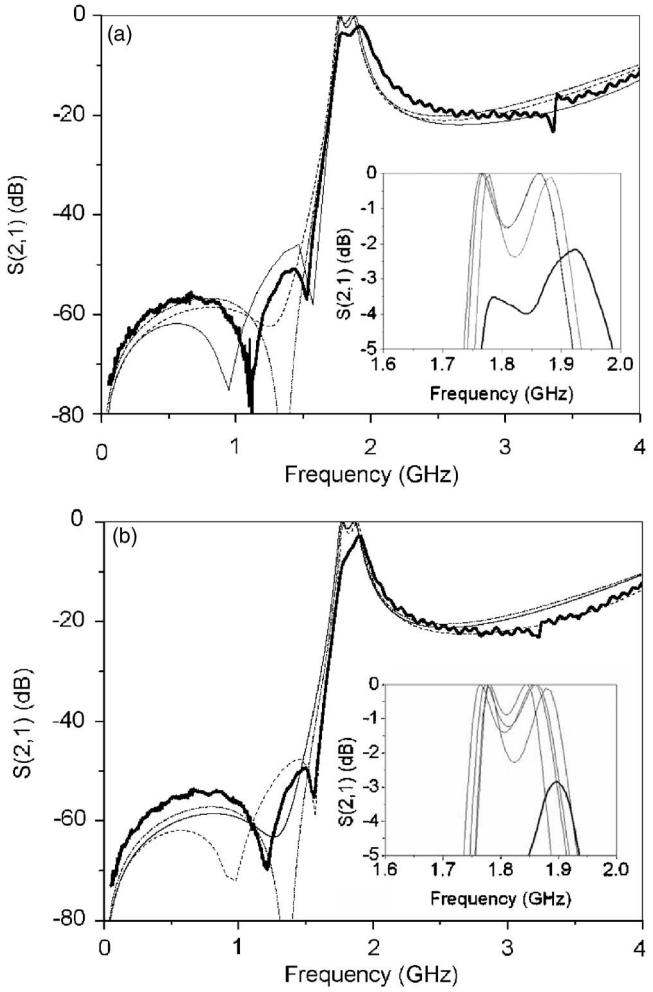

FIG. 10. Transmission coefficients for the circuits of Fig. 9 with inter-resonator distances of 0.1 mm (a) and 0.2 mm (b). Experimental response (bold line), full wave electromagnetic simulation (thin line), and electrical simulation by using the models shown in Fig. 4(a) (dotted line) and Fig. 5 (dash-dotted line) are depicted. In both cases, the transmission coefficient of the same structure excluding coupling (dotted bold line) has been included in order to check the influence of coupling (inset). Electrical parameters are L_r=1.6 nH, C_r=4.1 pF, C_c=4.6 pF, C_g=0.26 pF, L=5 nH, and (a) C_M =0.07 pF and (b) C_M=0.06 pF.

(this frequency response is also depicted in Fig. 8). As can be seen, the electrical model describes the electromagnetic behavior of the elemental cell to a very good approximation.

The following step has been used to fabricate several prototypes with different separations (and hence couplings) between CSRRs (two-stage devices have been implemented in all the cases to easy comparison). As in the previous single cell structure (Fig. 7), rectangular CSRRs have been etched in the ground plane in order to enhance electric coupling between CSRRs. The mutual capacitance C_M has been considered as a fitting parameter, and the capacitance of the CSRR C_r has been corrected (by subtracting C_M) to take into account the presence of the neighbor CSRRs.[32] In Figs. 9 and 10, the layouts and measured frequency responses (transmission coefficients) of the fabricated structures are depicted, as well as the electrical simulations of their equivalent circuit models [Figs. 4(a) and 5]. For the device with smaller inter-resonator distance (0.1 mm), coupling is higher, as revealed by the value of the mutual capacitance (0.07 pF). However, the differences are not substantial (C_M=0.06 pF for the device with 0.2 mm separation) and the frequency responses are similar. Two clearly identifiable transmission peaks arise in the allowed band. The accuracy of the model of Fig. 4(a) is good in all the cases, namely, since parameter extraction has been done from electromagnetic simulations, the electrical model of Fig. 4(a) fits very well the simulated frequency response. The simplified model of Fig. 5 also provides a good description of the structure, as expected on account of the results of Fig. 6, where it was demonstrated that the simplified model can be used up to coupling levels characterized by a mutual capacitance of roughly 0.2 pF, i.e., above the values that have been obtained for the two considered structures. Agreement between simulations and measurement is also good. The discrepancies are attributed to losses, not included in the simulations, and to fabrication related tolerances (dimensions are close to the resolution limits of our drilling machine). The authors would also like to mention that although inter-resonator coupling is moderate, this is significant and must be taken into account to provide an accurate description of the structure. To corroborate this, we have also obtained the electrical simulation of the model of Fig. 4(a) by neglecting the mutual capacitance. The result is depicted in the insets of Fig. 10 for the two considered structures. As can be seen, bandwidth is clearly narrower when coupling is excluded and the model does not provide an ac-

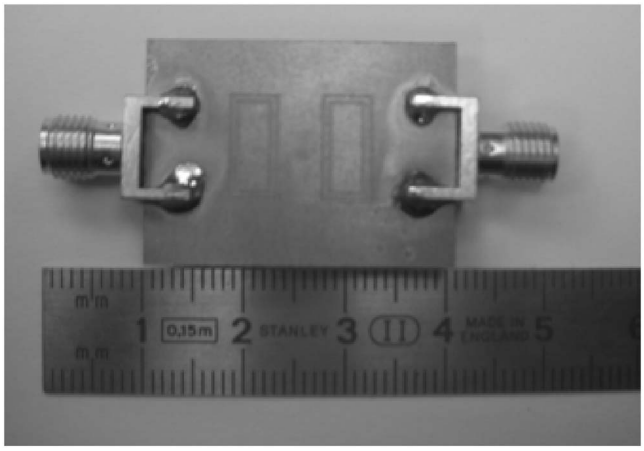

FIG. 11. Fabricated two-stage CSRR-based structure with rectangular CSRRs separated by 4.0 mm.

curate description of the frequency response. Hence, these results demonstrate that for structures with rectangular CSRRs separated by a small distance, (i) coupling must be taken into account in the circuit model, (ii) the circuit model describes the frequency response to a very good approximation, and (iii) the structure can be described by means a simplified equivalent circuit model, where the effects of inter-resonator coupling are accounted for by modifying the elements of the series branch. As will be shown in the last section (prior to conclusions), this is interesting to analytically obtain the dispersion relation of an infinite structure composed of these basic cells.

IV. EFFECTS OF CSRR SHAPE AND SEPARATION: WEAK COUPLING

Let us now consider two types of left handed structures: those where the distance between adjacent resonators (and hence the period) is comparable to signal wavelength at resonance and those where the CSRRs are circular. In the former case (see Fig. 11), inter-resonator coupling is negligible, but transmission line effects must be taken into account not only by the presence of the line inductance L but also by considering the line capacitance C which cannot be neglected provided that there is a significant portion of the line outside the

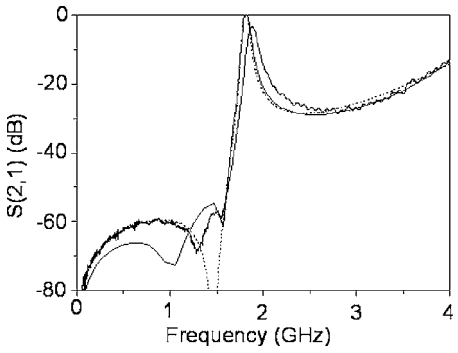

FIG. 12. Transmission coefficient for the circuit of Fig. 11. Experimental response (bold line), full wave electromagnetic simulation (thin line), and electrical simulation by using the model shown in Fig. 3 (dotted line) are depicted. L_r=1.6 nH, C_r=4.1 pF, C_c=4.5 pF, C_g=0.26 pF, L=5.2 nH, C=0.25 pF, and C_M=0 pF.

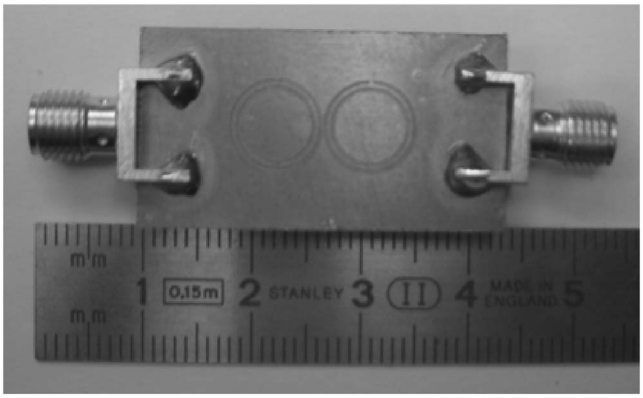

FIG. 13. Fabricated two-stage CSRR-based structure with circular CSRRs separated by a small distance (0.2 mm).

area region covered by the CSRRs. This has been verified by comparing the electrical simulation of the structure (Fig. 3) and the full wave electromagnetic simulation. To fit adequately both curves, it has been necessary to include the above cited capacitance (C) in the electrical model. The results are depicted in Fig. 12, together with the measured transmission coefficient. As compared to the structures of Fig. 9, only one transmission peak is visible in the device of Fig. 11, this being consequence of the lack of electric coupling between resonators. The excellent agreement between the electromagnetic simulation and the electrical simulation of the circuit of Fig. 3 is noteworthy.

For circular CSRRs separated by small distances (Fig. 13), the line capacitance does not play a role and can be neglected. However, since adjacent CSRRs are not coupled by an edge capacitance, coupling between them is very weak, as revealed by the value of the mutual capacitances resulting from the fitting of the electrical response to the full wave electromagnetic simulation (Fig. 14). Thus, in the previous electrical models of CSRR-based left handed and negative permeability microstrip lines, the exclusion of C_M (and hence coupling between resonators) is perfectly justified. Again, agreement between measurement, electromagnetic simulation, and electrical simulation is good. So, the general model for CSRR loaded microstrip lines depicted in Fig. 3 has been validated under different conditions, corresponding to different coupling levels between resonators, as

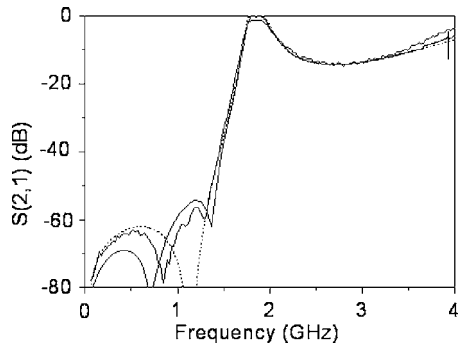

FIG. 14. Electromagnetic simulation (thin line), measured (bold line), and electrical simulation (dotted line) of the transmission coefficient for the structure depicted in Fig. 13 (L_r=2.7 nH, C_r=1.9 pF, C_c=5.3 pF, C_g=0.31 pF, L=4.5 nH, and C_M=0 pF).

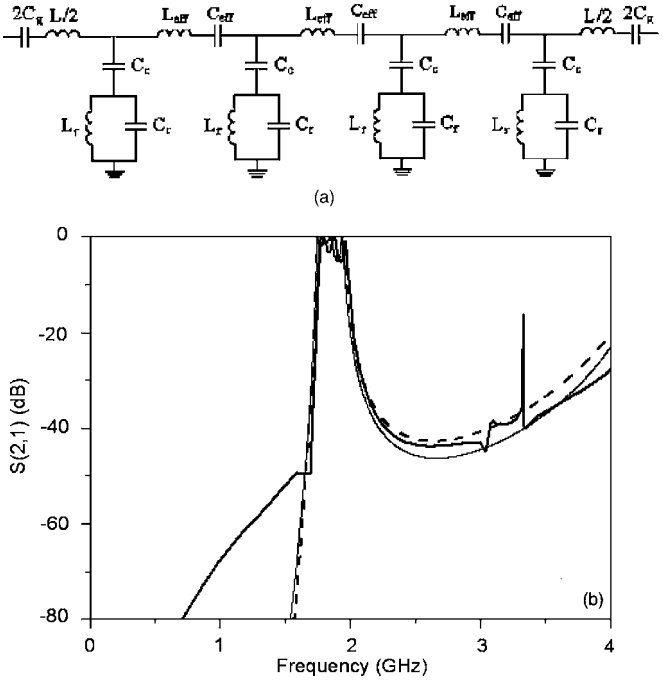

FIG. 15. Simplified equivalent circuit model for a four-stage device (a) and transmission coefficient (b). Comparison between the electromagnetic simulation (bold line), electrical simulation based on the exact model of Fig. 4(a) (thin line), and the simplified model (Fig. 5) is given. L_{eff}=3.97 nH, C_{eff} =0.37 pF, and C_M=0.07 pF.

well as resonator's shape. We would like to mention that the main aim of this work has been to obtain a general and accurate circuit model for CSRR-based left handed structures. This is of interest for the design of planar microwave circuits based on these types of artificial transmission lines. However, an accurate derivation of the element values from the geometry of the structure and its physical parameters (substrate permittivity and thickness) is complicated. For instance, a model that provides the electrical parameters of the CSRRs has been proposed by some of the authors,[30] but its validity is limited to some specific situations, which do not always correspond to practical applications. Therefore, for design purposes, a good method for parameter extraction from full wave simulation (as has been explained before) is necessary. Layout optimizers, such as those present in some commercial electromagnetic solvers (i.e., Agilent MOMENTUM), are also necessary for accurate circuit design.

V. THE DISPERSION RELATION

The previous analysis has been limited to two-stage devices, since under these conditions two visible transmission peaks typically arise in the frequency response, and these are good conditions to validate the circuit model. However, in practice, left handed structures may be realized by cascading a larger number of cells. Under these conditions, the analysis carried out in the Appendix [that has led us to the circuit of Fig. 4(g)] is not strictly valid. The reason is that in that analysis, each resonator is only coupled to the other, and this allows us to apply the Δ-Y equivalence. For a structure with more than two cells, each resonator (except those at the extremes) is coupled to the preceding and following one, and

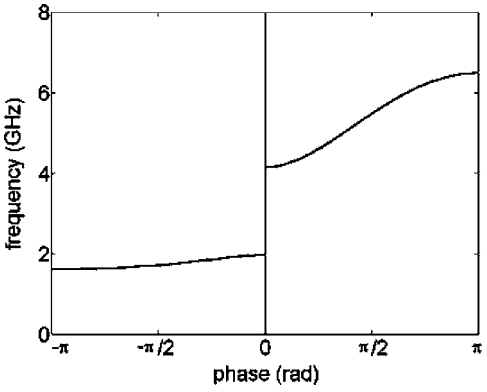

FIG. 16. Dispersion relation for the structure of Fig. 15.

we cannot proceed as described in the Appendix. Nevertheless, since coupling between resonators is not extreme (even under the more favorable conditions), it is expected that no substantial discrepancies between the model of Fig. 4(a) (extended to the required number of stages) and the model depicted in Fig. 5 arise. In other words, if coupling between a resonator's pair does not substantially influence adjacent coupling, which is reasonable at low and moderate coupling levels, the structure can be described to a good approximation by means of the model of Fig. 5 extended to the required number of stages. This has been corroborated by considering a four-stage structure (Fig. 15), where we have compared the electromagnetic simulation, the electrical simulation of the model of Fig. 4(a), and the electrical simulation of the model of Fig. 5. The agreement is again very good, which means that the simplified model can also be generalized to structures with more than two cells. We have used the model of Fig. 5 to obtain the dispersion relation [by means of expression (4)] of the structure (Fig. 16), where the typical features of left handed transmission line are visible, namely, a passband with backward wave propagation at low frequencies, as revealed by the antiparallelism between the phase and group velocities. At higher frequencies, an allowed band with the characteristics of forward wave propagation is also present and it is consequence of the elements of the host line.

VI. CONCLUSIONS

In conclusion, we have provided an exhaustive analysis of left handed microstrip lines loaded with complementary split rings resonators. Specifically, we have proposed a circuit model that takes into account inter-resonator coupling and line effects. The model has been found to provide a very good description of the structures under different conditions. It has been found that coupling is only relevant if square shaped CSRRs separated by a small distance are used. For the typical coupling levels obtained, it has been found that the equivalent circuit model can be simplified to a circuit where coupling effects are taken into account by simply modifying the line inductance and the gap capacitance, i.e., formally identical to previous models reported by the authors to describe structures with negligible coupling. For structures with circular CSRRs, coupling has been found to be negligible regardless of the inter-resonator distance, and this has been attributed to the limited edge capacitance when circular

topology is used. We have extended the simplified model, mathematically justified by considering two-stage devices, to structures with arbitrary number of stages and we have used this model to infer the dispersion relation, which has been found to exhibit the characteristics of left handed lines. The main conclusions of this work have been validated by comparing the results of the model with experimental results obtained from fabricated samples. In the opinion of the authors, this work represents a further step on the comprehension of the rich phenomenology associated with one-dimensional left handed structures based on resonant elements.

ACKNOWLEDGMENTS

This work has been supported by MEC (Spain) by project Contract Nos. TEC2004-04249-C02-01 and TEC2004-04249-C02-02 and by the European Commission through the Network of Excellence NoE 500252-2 METAMORPHOSE.

APPENDIX

To derive the circuit of Fig. 4, the Δ-Y equivalence is used. Let us express the circuit of Fig. 4(a) in the form shown in Fig. 4(b), where

$$Z_s = \frac{1}{j\omega C_g} + L\omega j, \tag{A1}$$

$$Z_C = \frac{1}{j\omega C_C}, \tag{A2}$$

$$Z_M = \frac{1}{j\omega C_M}, \tag{A3}$$

$$Z_r = \frac{j\omega L_r}{1-\omega^2 L_r C_r}. \tag{A4}$$

By using the Δ-Y equivalence, this circuit can be transformed to that shown in Fig. 4(c), where

$$Z_{12} = \frac{Z_C Z_r + Z_r Z_M/2 + Z_C Z_M/2}{Z_M/2} = j\frac{L_r(C_C + 2C_M + C_r)\omega^2 - 1}{C_C\omega(1-\omega^2 L_r C_r)}, \tag{A5}$$

$$Z_{23} = \frac{Z_C Z_r + Z_r Z_M/2 + Z_C Z_M/2}{Z_C} = j\frac{L_r(C_C + 2C_M + C_r)\omega^2 - 1}{2C_M\omega(1-\omega^2 L_r C_r)}, \tag{A6}$$

$$Z_{13} = \frac{Z_C Z_r + Z_r Z_M/2 + Z_C Z_M/2}{Z_r} = j\frac{1 - L_r(C_C + 2C_M + C_r)\omega^2}{2C_C C_M \omega^3 L_r}, \tag{A7}$$

and

$$Z' = \frac{Z_{23}}{2}. \tag{A8}$$

Finally, the Y configuration of the circuit of Fig. 4(d) can be expressed as shown in the circuit of Fig. 4(e), which is equivalent to that shown in Fig. 4(f), where

$$Z'_{12} = \frac{Z_{13}^2 + 2Z_{13}Z'}{Z'}, \tag{A9}$$

$$Z'_{23} = \frac{Z_{13}^2 + 2Z_{13}Z'}{Z_{13}}, \tag{A10}$$

$$Z'_{13} = \frac{Z_{13}^2 + 2Z_{13}Z'}{Z_{13}}, \tag{A11}$$

and

$$Z_P = \frac{Z_{12}Z'_{13}}{Z_{12} + Z'_{13}} = j\frac{\omega^2 L_r(C_C + C_r) - 1}{C_C\omega(1-\omega^2 L_r C_r)}, \tag{A12}$$

$$Z_{\text{eq}} = \frac{Z_s Z'_{12}}{Z_s + Z'_{12}}, \tag{A13}$$

so that the circuit of Fig. 4(g) is finally obtained, which is identical to the circuit of Fig. 4(a) by excluding coupling, and the series impedance modified and given by expression (1).

[1] D. R. Smith, W. J. Padilla, D. C. Vier, S. C. Nemat-Nasser, and S. Schultz, Phys. Rev. Lett. **84**, 4184 (2000).
[2] A. A. Oliner, URSI Digest, IEEE-AP-S USNC/URSI National Radio Science Meeting, San Antonio, TX, 2002 (unpublished), p. 41.
[3] C. Caloz and T. Itoh, Proceedings of the IEEE-AP-S USNC/URSI National Radio Science Meeting, San Antonio, TX, 2002 (unpublished), Vol. 2, p. 412.
[4] A. Grbic and G. V. Eleftheriades, J. Appl. Phys. **92**, 5930 (2002).
[5] R. Marqués, J. Martel, F. Mesa, and F. Medina, Phys. Rev. Lett. **89**, 183901 (2002).
[6] R. A. Shelby, D. R. Smith, S. C. Nemat-Nasser, and S. Schultz, Appl. Phys. Lett. **78**, 489 (2001).
[7] G. V. Eleftheriades, A. K. Iyer, and P. C. Kremer, IEEE Trans. Microwave Theory Tech. **50**, 2702 (2002).
[8] A. Grbic and G. V. Eleftheriades, J. Appl. Phys. **98**, 043106 (2005).
[9] R. A. Shelby, D. R. Smith, and S. Schultz, Science **292**, 77 (2001).
[10] C. G. Parazzoli, R. B. Greegor, K. Li, B. E. C. Koltenbah, and M. Tanielian, Phys. Rev. Lett. **90**, 107401 (2003).
[11] A. A. Houck, J. B. Brock, and I. L. Chuang, Phys. Rev. Lett. **90**, 137401 (2003).
[12] J. B. Pendry, Phys. Rev. Lett. **85**, 3966 (2000).
[13] N. García and M. Nieto-Vesperinas, Phys. Rev. Lett. **88**, 207403 (2002).
[14] G. Gómez-Santos, Phys. Rev. Lett. **90**, 077401 (2003).
[15] D. R. Smith, D. Schurig, M. Rosenbluth, S. Shultz, S. Annanta-Ramakrishna, and J. B. Pendry, Appl. Phys. Lett. **82**, 1506 (2003).
[16] R. Marqués and J. Baena, Microwave Opt. Technol. Lett. **41**, 290 (2004).
[17] C. Caloz and T. Itoh, *Electromagnetic Metamaterials: Transmission Line Theory and Microwave Applications* (Wiley, New York, 2005).
[18] V. G. Veselago, Sov. Phys. Usp. **10**, 509 (1968).
[19] J. B. Pendry, A. J. Holden, D. J. Robbins, and W. J. Stewart, IEEE Trans. Microwave Theory Tech. **47**, 2075 (1999).
[20] R. Marqués, F. Mesa, J. Martel, and F. Medina, IEEE Trans. Antennas Propag. **51**, 2572 (2003).
[21] R. Marqués, J. D. Baena, J. Martel, F. Medina, F. Falcone, M. Sorolla, and F. Martín, Proceedings of the ICEAA'03, Torino, Italy, 2003 (unpublished), p. 439.
[22] J. D. Baena, R. Marqués, F. Medina, and J. Martel, Phys. Rev. B **69**, 014402 (2004).
[23] J. García-García, F. Martín, J. D. Baena, and R. Maqués, J. Appl. Phys.

98, 033103 (2005).
[24]I. Bahl and P. Bhartia, *Microwave Solid State Circuit Design* (Wiley, Toronto, 1988).
[25]C. Caloz and T. Itoh., *IEEE-MTT International Symposium, Philadelphia, PA, 8–13 June 2006* (IEEE, New York, 2003), Vol. 1, p. 195.
[26]A. Sanada, C. Caloz, and T. Itoh, IEEE Microw. Wirel. Compon. Lett. **14**, 68 (2004).
[27]F. Martín, F. Falcone, J. Bonache, R. Marqués, and M. Sorolla, Appl. Phys. Lett. **83**, 4652 (2003).
[28]F. Falcone, T. Lopetegi, M. A. G. Laso, J. D. Baena, J. Bonache, R. Marqués, F. Martín, and M. Sorolla, Phys. Rev. Lett. **93**, 197401 (2004).
[29]F. Falcone, T. Lopetegi, J. D. Baena, R. Marqués, F. Martín, and M. Sorolla, IEEE Microw. Wirel. Compon. Lett. **14**, 280 (2004).
[30]J. D. Baena *et al.*, IEEE Trans. Microwave Theory Tech. **53**, 1451 (2005).
[31]J. García-García *et al.*, IEEE Trans. Microwave Theory Tech. **53**, 1997 (2005).
[32]M. Beruete, M. J. Freire, R. Marqués, F. Falcone, and J. D. Baena, Appl. Phys. Lett. **88**, 083503 (2006).
[33]E. Shamonina, V. A. Kalinin, K. H. Ringhofer, and L. Solymar, J. Appl. Phys. **82**, 6252 (2002).
[34]M. C. K. Wiltshire, E. Shamonina, I. R. Young, and L. Solymar, Electron. Lett. **39**, 215 (2003).
[35]M. J. Freire, R. Marqués, F. Medina, M. A. G. Laso, and F. Martín, Appl. Phys. Lett. **85**, 4439 (2004).
[36]R. R. A. Syms, E. Shamonina, and L. Solymar, J. Appl. Phys. **97**, 064909 (2005).
[37]J. Bonache, M. Gil, I. Gil, J. Garcia-García, and F. Martín, IEEE Microw. Wirel. Compon. Lett. (to be published).
[38]D. M. Pozar, *Microwave Engineering* (*Addison-Wesley*, Reading, MA, 1990).